




Atomic layer deposition of a MgO barrier for a passivated black phosphorus spintronics platform

Cite as: Appl. Phys. Lett. **114**, 053107 (2019); <https://doi.org/10.1063/1.5086840>

Submitted: 24 December 2018 . Accepted: 23 January 2019 . Published Online: 07 February 2019

L.-M. Kern , R. Galceran, V. Zatzko, M. Galbiati, F. Godel, D. Perconte, F. Bouamrane, E. Gaufrès, A. Loiseau, P. Brus, O. Bezencenet, M.-B. Martin, B. Servet, F. Petroff , B. Dlubak , and P. Seneor



View Online



Export Citation



CrossMark

ARTICLES YOU MAY BE INTERESTED IN

[Perpendicular magnetic anisotropy and spin mixing conductance in polycrystalline europium iron garnet thin films](#)

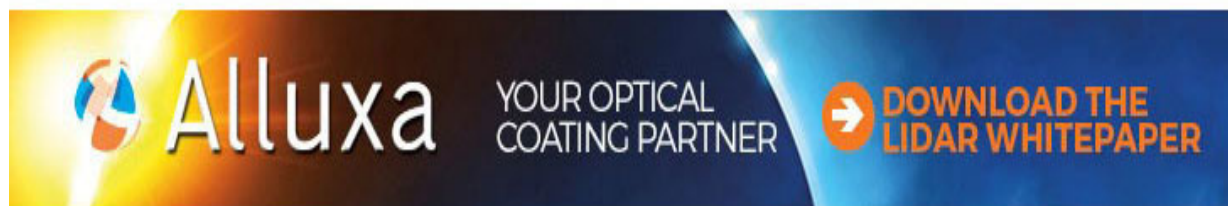
Applied Physics Letters **114**, 052403 (2019); <https://doi.org/10.1063/1.5074166>

[Heteroepitaxy of MoSe₂ on Si\(111\) substrates: Role of surface passivation](#)

Applied Physics Letters **114**, 053106 (2019); <https://doi.org/10.1063/1.5083974>

[Role of hybridization and magnetic effects in massive Dirac cones: Magnetic topological heterostructures with controlled film thickness](#)

Applied Physics Letters **114**, 051602 (2019); <https://doi.org/10.1063/1.5083059>



Atomic layer deposition of a MgO barrier for a passivated black phosphorus spintronics platform

Cite as: Appl. Phys. Lett. **114**, 053107 (2019); doi: [10.1063/1.5086840](https://doi.org/10.1063/1.5086840)

Submitted: 24 December 2018 · Accepted: 23 January 2019 ·

Published Online: 7 February 2019



View Online



Export Citation



CrossMark

L.-M. Kern,¹  R. Galceran,¹ V. Zatko,¹ M. Galbiati,¹ F. Godel,¹ D. Perconte,¹ F. Bouamrane,¹ E. Gaufrès,² A. Loiseau,² P. Brus,³ O. Bezencenet,³ M.-B. Martin,³ B. Servet,³ F. Petroff,¹  B. Dlubak,^{1,a)}  and P. Seneor^{1,a)}

AFFILIATIONS

¹Unité Mixte de Physique, CNRS, Thales, University Paris-Sud, Université Paris-Saclay, 91767 Palaiseau, France

²Laboratoire d'Étude des Microstructures (LEM), CNRS, ONERA, Université Paris-Saclay, 92322 Châtillon, France

³Thales Research and Technology, 1 avenue Augustin Fresnel, 91767 Palaiseau, France

^{a)} Authors to whom correspondence should be addressed: bruno.dlubak@cnsr-thales.fr and pierre.seneor@cnsr-thales.fr

ABSTRACT

We demonstrate a stabilized black phosphorus (BP) 2D platform thanks to an ultrathin MgO barrier, as required for spintronic device integration. The *in-situ* MgO layer deposition is achieved by using a large-scale atomic layer deposition process with high nucleation density. Raman spectroscopy studies show that this layer protects the BP from degradation in ambient conditions, unlocking in particular the possibility to carry out usual lithographic fabrication steps. The resulting MgO/BP stack is then integrated in a device and probed electrically, confirming the tunnel properties of the ultrathin MgO contacts. We believe that this demonstration of a BP material platform passivated with a functional MgO tunnel barrier provides a promising perspective for BP spin transport devices.

© 2019 Author(s). All article content, except where otherwise noted, is licensed under a Creative Commons Attribution (CC BY) license (<http://creativecommons.org/licenses/by/4.0/>). <https://doi.org/10.1063/1.5086840>

Black Phosphorus (BP) is a very promising material for spintronics, with expected intrinsically low spin orbit-coupling¹ and reported large mobilities.^{2–5} Since its recent renaissance, BP has thus been seen as a material with strong potential for long distance spin transport. Furthermore, compared to graphene, BP possesses a tunable bandgap.^{2–4} This could prove a pivotal asset for the control of spin flows in envisioned spin logic architectures.^{6–8} Hence, while this material has been only recently put forward, few pioneering results on BP integration for spintronics, either in lateral spin valves⁹ or in vertical 2D-Magnetic Tunnel Junctions,¹⁰ have already been reported. However, as noted before in diverse cases of channel materials (e.g., Si,¹¹ GaAs,¹² nanotubes,^{13,14} graphene^{15,16}...), efficient spin injection in a resistive/semiconducting material such as BP is known to be particularly difficult. Indeed, the spin device performances are dependent on device parameters beyond the sole BP intrinsic spin transport properties. It is for instance, well understood that a direct or a poorly controlled tunnel contact between a metallic ferromagnetic spin source and the semiconducting channel leads to spin back-flow, artificially quenching the injected spin's lifetimes.^{17–19} Harnessing BP spin properties requires thus to

integrate it with a high-quality interfacial tunnel barrier. This has been proved to be particularly challenging to engineer. The main difficulty is that BP suffers from a rapid photo-oxidation reaction in ambient conditions with a strong impact on transport properties:²⁰ it degrades almost immediately,²¹ forbidding any further fabrication and characterization of a pristine BP device. In this context, it appears that investigations of multi-functional passivation approaches are required. Unfortunately, it has been shown that wetting continuous ultrathin layers on 2D materials (which provide no dangling bonds) is particularly difficult, especially with soft processes such as atomic layer deposition (ALD).^{22,23} Hence, BP spin studies require as a foundational step the identification of fabrication protocols leading to both protection and ultrathin tunnel contacts, in order to further unlock efficient spin transport devices.

In this letter, we present a simple process which provides both a passivation barrier for the BP spin transport channel and a tunnel barrier required for spin injection. We make use of a large scale *in-situ* ALD process (Fig. 1) developed to allow full wetting of ultra-thin oxides on 2D materials and derive a continuous MgO barrier (Fig. 2). Thanks to this ALD grown passivation

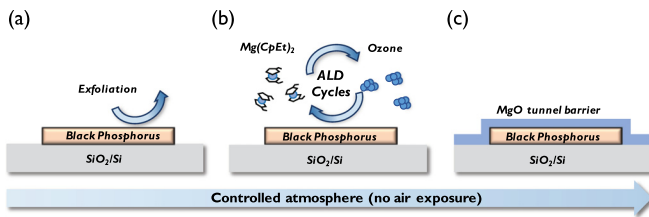


FIG. 1. MgO tunnel barrier ALD growth process. (a) Black Phosphorus flakes are exfoliated in a glovebox. (b) Using a sealed suitcase, samples are transferred in the ALD setup and precursor cycles are carried out resulting in (c) a 3 nm MgO tunnel barrier on BP.

layer, the black phosphorus flakes are shown to remain pristine, even after over 1 month in ambient conditions (Fig. 3). Crucially, we demonstrate the use of this ultra-thin MgO capping layer as an efficient tunnel barrier for BP devices (Fig. 4) further highlighting the potential of this stabilized platform for spintronics.

In Fig. 1, we describe the particular *in-situ* process that we carry out to passivate BP flakes with a MgO barrier. First, the flakes are derived onto a SiO₂(90 nm)/Si substrate from a BP bulk crystal using the mechanical exfoliation method. Working in an ambient atmosphere, as is usually the case for graphene exfoliation,²⁴ is not adapted for BP. Indeed, BP is extremely sensitive to the combined action of oxygen, humidity, and light.^{21,25} In particular, exposure to ambient conditions leads to a strong and rapid degradation: BP flakes react almost immediately to form phosphoric acid droplets.^{21,25} Thus, for our process, the exfoliation steps are carried out under a controlled atmosphere inside a glovebox [Fig. 1(a)] where the H₂O and O₂ levels are kept below 1 ppm. Once exfoliated, BP layers cannot be taken out in air as such for further processing; an *in-situ* passivation step is necessary. The prepared BP samples are transferred to the ALD growth chamber in a controlled inert atmosphere using a transfer suitcase. The suitcase is closed while in the glovebox allowing to maintain the samples in an atmosphere with <1 ppm of H₂O

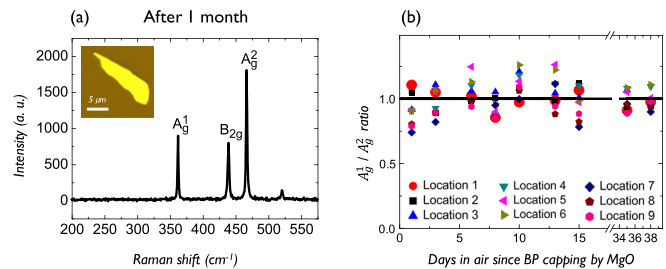


FIG. 3. Raman characterization of MgO passivated flakes after extended period in air. (a) Main BP Raman signatures are shown after 1 month in air. (b) No significant change is recorded for the normalized Raman A_g¹/A_g² ratio during a 1+ month study, revealing the stabilization of the structural properties of the BP flakes. This is in strong contrast with bare unprotected flakes where no BP peaks are visible after rapid degradation.

and O₂. The closed suitcase is then hermetically sealed on a docking port of the load-lock of the ALD system and opened only once the load-lock is pumped down to vacuum. This allows a transfer of the BP samples to the growth chamber without any air exposure. The ALD process is then performed on the BP samples using cycles of magnesium precursor Mg(EtCp)₂ [bis(ethyl-cyclopentadienyl)magnesium] and ozone to achieve a conformal MgO layer [Fig. 1(b)]. The Mg(EtCp)₂ is heated at 50 °C to enhance its vapor pressure and pushed in the chamber with pulsed N₂ flow assistance. The growth is carried out at a relatively low chamber temperature of 100 °C to maximize wetting efficiency.^{23,26} As such, our process leads to the growth of 3 nm of MgO [Fig. 1(c)] as confirmed by ellipsometry. Below, we demonstrate the continuity of this ultra-thin film and thus its possible use as both passivation and tunnel barriers.

To illustrate the pertinence of our ozone based ALD process on BP, we present in Fig. 2 a set of Scanning Electron Microscope (SEM) pictures of BP flakes after 3 different processes. First, as a reference to show the particular sensitivity of BP in air, Fig. 2(a) reveals the degradation of unprotected bare

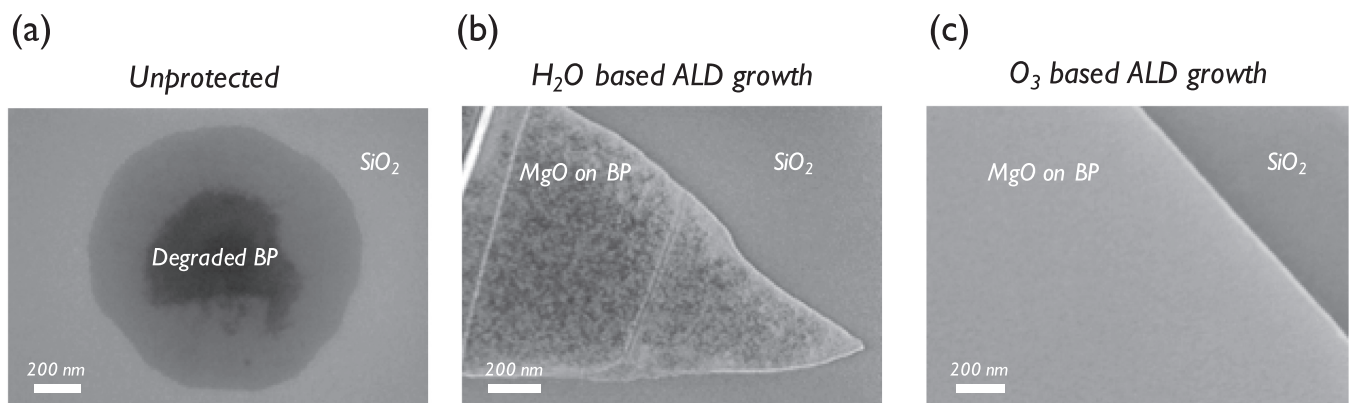


FIG. 2. SEM imaging of BP flakes prepared in different conditions. (a) Bare BP flakes exposed to air start degrading almost immediately and end up in the form of phosphoric acid droplets. (b) Using a water based *in-situ* ALD process does not fully wet the BP flake and results in a discontinuous MgO layer. These samples have been carefully transferred to the SEM just after the deposition to allow a good evaluation of the MgO coverage before any strong BP degradation. After being left longer in air, the flakes underwent leaking similar to (a). (c) Direct *in-situ* ozone-based ALD of MgO allows an extremely homogeneous wetting on the BP flake. No droplet is observed for these samples even after an extended period in air.

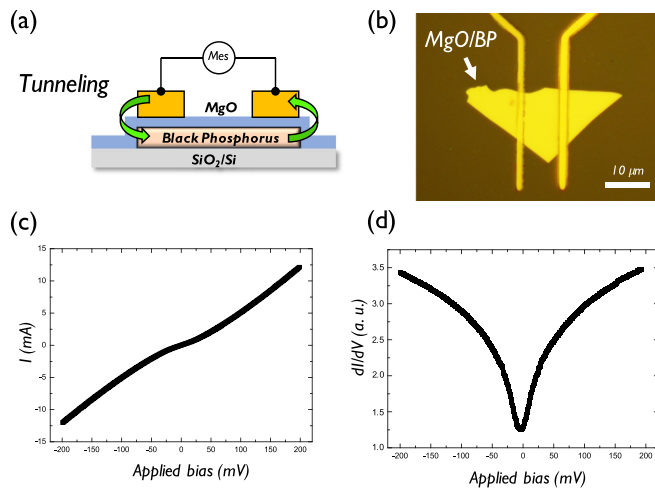


FIG. 4. (a) A lateral device is fabricated with two tunnel contacts on the BP flake through the MgO tunnel barrier. (b) An optical picture of the device is displayed (scale bar is 10 μm). (c) The measured $I(V)$ and (d) $dI/dV(V)$ curves show typical characteristics of tunnel injection in the BP channel.

BP when it is exposed to ambient conditions. Degradation starts immediately upon air exposure and leads to a droplet-like material for most of the flakes on the timescale of a day. It is clearly seen that the reactivity with air destroys BP structural properties, highlighting the crucial need for passivation. Figure 2(b) shows the attempt of a passivation of BP with magnesium oxide deposited by ALD using H₂O as one of the precursors instead of ozone. A discontinuous film is revealed after growth: the water based ALD is insufficient to correctly wet the surface of BP. This is reminiscent of previous studies of ALD on different 2D materials,²³ where the absence of dangling bonds on the 2D surface was shown to prevent the fixation of precursors, leading to very low wetting. In our case, as we target film thicknesses on the nm scale, we cannot afford to use a seed layer to promote the wetting of films grown by water-based ALD, as usually suggested.^{27–31} Overall, the water-based processes commonly used in the literature appear unsuited for ultrathin barrier growth on BP. We further note that the BP flakes covered with this discontinuous MgO layer underwent degradation when left in air, similar to uncovered flakes. In Fig. 2(c), we make use of the ozone based ALD process. The choice of ozone (vs more usual water-based processes) is thus dictated by this difficulty to grow continuous ultra-thin layers by ALD on 2D materials.^{29,32} Similar to the previously discussed case of the ozone-based growth of Al₂O₃ on graphene,²⁶ ozone adsorption is key to enable the full wetting during first cycles and enable the growth of continuous films even at nm thicknesses. The resulting wetting is strikingly different. In clear contrast with the water-based process [Figs. 2(b) vs 2(c)], the film appears to fully wet the surface. We observe no degradation or droplet formation thanks to this MgO barrier on a long observation period, as detailed below. The use of ozone adsorption on the surface is thus shown to be key in order to derive continuous ultrathin films on BP by ALD.

The effective passivation of BP thanks to the MgO barrier is demonstrated in Fig. 3. We carried out a Raman spectroscopy study over an extended period of time on 9 different locations. We focus here on a set of flakes with thicknesses between 5 nm and 60 nm, as characterized by AFM. However, we observed similar evolution for any derived flake. Passivated BP flakes are left in air for over one month, with regular Raman analysis of their crystalline state. The vibrational modes A_g^1 , A_g^2 , and B_{2g} (as well as the Si substrate peak)²¹ appear on the Raman spectra taken on BP flakes, as shown in Fig. 3(a). This is already meaningful as, if unprotected BP is left in air, these signature peaks disappear on a time scale well below 1h, while the Raman spectrum shown in Fig. 3(a) is taken after 1 month in air. Furthermore, no significant evolution of the Raman spectra is observed over time. In particular, the ratio between the amplitudes of A_g^1 and A_g^2 modes indicating the degree of degradation of BP^{21,33} does not present any remarkable evolution as shown in Fig. 3(b) for the 9 tracked locations. These results show the robust passivation of BP with our ultrathin MgO barrier obtained by ALD. Using our *in-situ* exfoliation and passivation method, we are now able to take the BP layers *ex-situ* and undertake any required further processing towards device integration.

In this direction, as shown in Fig. 4, we illustrate the pertinence of our passivation scheme by fabricating a full device and measuring the performance of the MgO ultrathin layer as a tunnel barrier. As shown in Figs. 4(a) and 4(b), we define two contact electrodes on top of the BP flake. These are fabricated by laser photo-lithography (Dilase 650 from Kloe) and lift-off steps after Co and NiFe deposition by sputtering, respectively, for each electrode. The conduction channel defined between the two electrodes has a length of 10 μm . A third lithography step is carried out to define gold bonding pads. An optical image of the resulting device is presented in Fig. 4(b). It is worth noting that the passivation is essential for such a fabrication scheme, and in its absence, all the flakes would have suffered severe degradation and would have been etched away. Thanks to our *in-situ* capping scheme, the BP flake has never been directly exposed to ambient conditions. Optical, AFM, and Raman observations show no noticeable change after fabrication. We further show a transport measurement in this device to demonstrate the use of our MgO thin film as a functional tunneling contact. In Figs. 4(c) and 4(d), we present I - V and dI/dV transport measurements in the device recorded at 4 K. As schematically depicted in Fig. 4(a), a current is injected through tunneling from the first electrode across the first MgO interface, propagating in the BP channel and tunneling through the second MgO interface to the second electrode. The $I(V)$ curve shows a non-linear behavior, and the first derivative dI/dV confirms this with a parabolic shape, a typical characteristic of tunneling contacts. The transport signatures measured in this device demonstrate the pertinence of our ALD based protocol. In particular, the high homogeneity (absence of pinhole) in the ALD grown MgO ultra-thin layer grants the stability of the BP flake and allows a well-defined tunneling behavior in devices.

In conclusion, we present in this study a large-scale ALD process to simultaneously passivate BP and provide a tunneling interface required for efficient spin injection. The MgO/BP

structure is derived *in-situ* to prevent any air exposure. The BP layer is shown to be stabilized over 1 month of observation, without noticeable structural evolution. Importantly, the passivation MgO layer is demonstrated to also behave as a functional tunnel barrier. We believe that this will prove to be a strong asset towards the use of BP for spintronics. Indeed, in addition to passivation, this ALD grown tunnel barrier will serve to mitigate the impedance mismatch issue between ferromagnets and the BP channel, as required in order to inject spin polarized current into BP.^{15,19}

The authors acknowledge funding from the European Union's FP7/Horizon 2020 research and innovation program under Grant Agreement Graphene Flagship (No. 696656) and from French Agence Nationale de la Recherche (ANR) Project EPOS-BP (ANR-17-CE24-0023-03).

REFERENCES

- ¹M. Kurpas, M. Gmitra, and J. Fabian, *J. Phys. D: Appl. Phys.* **51**, 174001 (2018).
- ²L. Li, Y. Yu, G. J. Ye, Q. Ge, X. Ou, H. Wu, D. Feng, X. H. Chen, and Y. Zhang, *Nat. Nanotechnol.* **9**, 372 (2014).
- ³J. Jia, S. K. Jang, S. Lai, J. Xu, Y. J. Choi, J.-H. Park, and S. Lee, *ACS Nano* **9**, 8729 (2015).
- ⁴G. Long, D. Maryenko, J. Shen, S. Xu, J. Hou, Z. Wu, W. K. Wong, T. Han, J. Lin, Y. Cai, R. Lortz, and N. Wang, *Nano Lett.* **16**, 7768 (2016).
- ⁵X. Ling, H. Wang, S. Huang, F. Xia, and M. S. Dresselhaus, *Proc. Natl. Acad. Sci. U. S. A.* **112**, 4523 (2015).
- ⁶B. Behin-Aein, D. Datta, S. Salahuddin, and S. Datta, *Nat. Nanotechnol.* **5**, 266 (2010).
- ⁷S. Manipatruni, D. E. Nikonov, and I. A. Young, *IEEE Trans. Circuits Syst.* **59**, 2801 (2012).
- ⁸S. Manipatruni, D. E. Nikonov, and I. A. Young, *Phys. Rev. Appl.* **5**, 014002 (2016).
- ⁹A. Avsar, J. Y. Tan, M. Kurpas, M. Gmitra, K. Watanabe, T. Taniguchi, J. Fabian, and B. Özyilmaz, *Nat. Phys.* **13**, 888 (2017).
- ¹⁰L. Xu, J. Feng, K. Zhao, W. Lv, X. Han, Z. Liu, X. Xu, H. Huang, and Z. Zeng, *Adv. Condens. Matter Phys.* **2017**, 9042823 (2017).
- ¹¹S. P. Dash, S. Sharma, R. S. Patel, M. P. de Jong, and R. Jansen, *Nature* **462**, 491 (2009).
- ¹²X. Lou, C. Adelmann, S. A. Crooker, E. S. Garlid, J. Zhang, K. S. M. Reddy, S. D. Flexner, C. J. Palmström, and P. A. Crowell, *Nat. Phys.* **3**, 197 (2007).
- ¹³L. E. Hueso, J. M. Pruneda, V. Ferrari, G. Burnell, J. P. Valdes-Herrera, B. D. Simons, P. B. Littlewood, E. Artacho, A. Fert, and N. D. Mathur, *Nature* **445**, 410 (2007).
- ¹⁴A. Anane, B. Dlubak, H. Idzuchi, H. Jaffres, M.-B. Martin, Y. Otani, P. Seneor, and A. Fert, *Handbook of Spintronics* (Springer Netherlands, Dordrecht, 2016), pp. 681–706.
- ¹⁵P. Seneor, B. Dlubak, M.-B. Martin, A. Anane, H. Jaffres, and A. Fert, *MRS Bull.* **37**, 1245 (2012).
- ¹⁶S. Roche, J. Åkerman, B. Beschoten, J.-C. Charlier, M. Chshiev, S. P. Dash, B. Dlubak, J. Fabian, A. Fert, M. Guimarães, F. Guinea, I. Grigorieva, C. Schönberger, P. Seneor, C. Stampfer, S. O. Valenzuela, X. Waintal, and B. Van Wees, *2D Mater.* **2**, 030202 (2015).
- ¹⁷G. Schmidt, D. Ferrand, L. Molenkamp, A. Filip, and B. van Wees, *Phys. Rev. B* **62**, R4790 (2000).
- ¹⁸A. Fert and H. Jaffrès, *Phys. Rev. B* **64**, 184420 (2001).
- ¹⁹A. Fert, J.-M. George, H. Jaffres, and R. Mattana, *IEEE Trans. Electron Devices* **54**, 921 (2007).
- ²⁰S. P. Koenig, R. A. Doganov, H. Schmidt, A. H. Castro Neto, and B. Özyilmaz, *Appl. Phys. Lett.* **104**, 103106 (2014).
- ²¹A. Favron, E. Gaufrès, F. Fossard, A.-L. Phaneuf-L'Heureux, N. Y.-W. Tang, P. L. Lévesque, A. Loiseau, R. Leonelli, S. Francoeur, and R. Martel, *Nat. Mater.* **14**, 826 (2015).
- ²²B. Dlubak, M.-B. Martin, C. Deranlot, K. Bouzehouane, S. Fusil, R. Mattana, F. Petroff, A. Anane, P. Seneor, and A. Fert, *Appl. Phys. Lett.* **101**, 203104 (2012).
- ²³B. Dlubak, P. R. Kidambi, R. S. Weatherup, S. Hofmann, and J. Robertson, *Appl. Phys. Lett.* **100**, 173113 (2012).
- ²⁴K. S. Novoselov, D. Jiang, F. Schedin, T. J. Booth, V. V. Khotkevich, S. V. Morozov, and A. K. Geim, *Proc. Natl. Acad. Sci. U. S. A.* **102**, 10451 (2005).
- ²⁵J. O. Island, G. A. Steele, H. S. J. van der Zant, and A. Castellanos-Gomez, *2D Mater.* **2**, 011002 (2015).
- ²⁶M.-B. Martin, B. Dlubak, R. S. Weatherup, H. Yang, C. Deranlot, K. Bouzehouane, F. Petroff, A. Anane, S. Hofmann, J. Robertson, A. Fert, and P. Seneor, *ACS Nano* **8**, 7890 (2014).
- ²⁷J. A. Robinson, M. LaBella, K. A. Trumbull, X. Weng, R. Cavelero, T. Daniels, Z. Hughes, M. Hollander, M. Fanton, and D. Snyder, *ACS Nano* **4**, 2667 (2010).
- ²⁸B. Fallahazad, S. Kim, L. Colombo, and E. Tutuc, *Appl. Phys. Lett.* **97**, 123105 (2010).
- ²⁹X. Wang, S. M. Tabakman, and H. Dai, *J. Am. Chem. Soc.* **130**, 8152 (2008).
- ³⁰D. B. Farmer, H.-Y. Chiu, Y.-M. Lin, K. A. Jenkins, F. Xia, and P. Avouris, *Nano Lett.* **9**, 4474 (2009).
- ³¹I. Meric, C. R. Dean, A. F. Young, N. Baklitskaya, N. J. Tremblay, C. Nuckolls, P. Kim, and K. L. Shepard, *Nano Lett.* **11**, 1093 (2011).
- ³²B. B. Burton, D. N. Goldstein, and S. M. George, *J. Phys. Chem. C* **113**, 1939 (2009).
- ³³A. Favron, F. A. Goudreault, V. Gosselin, J. Groulx, M. Côté, R. Leonelli, J.-F. Germain, A.-L. Phaneuf-L'Heureux, S. Francoeur, and R. Martel, *Nano Lett.* **18**, 1018 (2018).